Title

The Pol II preinitiation complex (PIC) influences Mediator binding but not promoter—enhancer looping

Journal

Genes & Development, 35(15-16)

ISSN

0890-9369

Authors

Sun, Fei
Sun, Terrence
Kronenberg, Michael
et al.

Publication Date

2021-08-01

DOI

10.1101/gad.348471.121

Peer reviewed

The Pol II preinitiation complex (PIC) influences Mediator binding but not promoter–enhancer looping

Fei Sun,[1] Terrence Sun,[1] Michael Kronenberg,[1] Xianglong Tan,[1] Chengyang Huang,[2] and Michael F. Carey[1]

[1]Department of Biological Chemistry, David Geffen School of Medicine at University of California at Los Angeles, Los Angeles, California 90095, USA; [2]Center for Neurobiology, Shantou University Medical College, Shantou 515041, China

Knowledge of how Mediator and TFIID cross-talk contributes to promoter–enhancer (P-E) communication is important for elucidating the mechanism of enhancer function. We conducted an shRNA knockdown screen in murine embryonic stem cells to identify the functional overlap between Mediator and TFIID subunits on gene expression. Auxin-inducible degrons were constructed for TAF12 and MED4, the subunits eliciting the greatest overlap. Degradation of TAF12 led to a dramatic genome-wide decrease in gene expression accompanied by destruction of TFIID, loss of Pol II preinitiation complex (PIC) at promoters, and significantly decreased Mediator binding to promoters and enhancers. Interestingly, loss of the PIC elicited only a mild effect on P-E looping by promoter capture Hi-C (PCHi-C). Degradation of MED4 had a minor effect on Mediator integrity but led to a consistent twofold loss in gene expression, decreased binding of Pol II to Mediator, and decreased recruitment of Pol II to the promoters, but had no effect on the other PIC components. PCHi-C revealed no consistent effect of MED4 degradation on P-E looping. Collectively, our data show that TAF12 and MED4 contribute mechanistically in different ways to P-E communication but neither factor appears to directly control P-E looping, thereby dissociating P-E communication from physical looping.

[*Keywords*: enhancer; promoter; Mediator; TFIID; chromatin looping; gene expression]

Supplemental material is available for this article.

Received March 18, 2021; revised version accepted June 24, 2021.

Eukaryotic transcription initiation is well understood biochemically and structurally, but many questions remain as to how sequence-specific activators at enhancers and promoters communicate with the machinery that guides RNA polymerase II (Pol II) to the transcription start site (TSS). Although the two major coactivator complexes, transcription factor IID (TFIID) and Mediator, enable Pol II preinitiation complex (PIC) assembly and function at the promoter, it is unclear how Mediator mechanistically stimulates transcription or how the PIC at a promoter communicates with Mediator bound at enhancers. It is evident that enhancers and promoters directly and dynamically interact, but it is unknown whether this interaction is driven by TFIID, Mediator, the PIC, or other factors. Knowledge of how the major coactivators function in cells is crucial to determine the precise mechanisms of gene activation.

TFIID is a general transcription factor (GTF) composed of TATA binding protein (TBP) and 13 TBP-associated factors (TAFs). It recognizes DNA elements constituting the core promoter encompassing the TSS (Bhuiyan and Timmers 2019). TFIID binding, which is enhanced by TFIIA, leads to recruitment of other GTFs including TFIIB, which in turn recruits Pol II associated with TFIIF (Buratowski et al. 1989). The presence of TFIIB is critical because it directly interacts with both the wall and cleft of Pol II (Kostrewa et al. 2009). Subsequently, TFIIE and TFIIH are recruited to enable formation and stabilization of the open complex (Holstege et al. 1996). Activators interact with TFIID to stabilize its binding to the core promoter and stimulate PIC assembly (Chi et al. 1995; Kuras and Struhl 1999). A small amount of TFIID is found at enhancers associated with noncoding transcription, but the bulk of it binds promoters (Koch et al. 2011). Although the assembly of the GTFs and Pol II has historically been considered the PIC, biochemical, structural, and genomic studies have shown that Mediator is a key PIC component (Soutourina 2018).

Corresponding author: mcarey@mednet.ucla.edu
Article published online ahead of print. Aricle and publication date are online at http://www.genesdev.org/cgi/doi/10.1101/gad.348471.121.

Mediator is a transcriptional coactivator found in all eukaryotes (Bourbon 2008). It is bound at both promoters and enhancers (Kagey et al. 2010). In yeast, Mediator was originally discovered in a holoenzyme with Pol II (Kim et al. 1994). In mammals, Mediator is composed of 30 subunits, which are structurally organized into four modules termed the head, middle, and tail (HMT), and the CDK8 kinase module (CKM). Mammalian Mediator exists in two major forms in nuclear extracts: one with HMT bound to CKM and the other with HMT bound to MED26 and Pol II (Sato et al. 2004). In biochemical studies, Mediator stimulates PIC assembly in an activator-dependent manner (Johnson and Carey 2003). Indeed, many activators interact directly with Mediator, often through subunits in the middle and tail modules. Mediator in turn promotes PIC assembly through direct interactions with Pol II and GTFs (Soutourina 2018). Pol II also makes major contacts with TFIIB (Kostrewa et al. 2009). Understanding the role of Mediator and TFIIB in Pol II recruitment is important for determining what drive the final levels of Pol II at a promoter, and the overall rate of transcription.

TFIID and Mediator interact physically in biochemical experiments and are thought to act coordinately to turn on genes. In humans, the Mediator subunit MED26 interacts with TFIID but also with elongation factors ELL/EAF and P-TEFb (Takahashi et al. 2011). Human TFIID and Mediator assemble cooperatively on promoters in reactions reconstituted with purified proteins (Johnson et al. 2002). In yeast, Mediator anchor-away leads to a modest decrease of TFIID binding at promoters, but loss of TFIID impairs Mediator recruitment at upstream activating sequences (UASs) (Grünberg et al. 2016).

Promoter–enhancer (P-E) interactions are believed to have a key role in stimulating transcription, but what drives the establishment of P-E loops has yet to be established. Cohesin, which binds CCCTC-binding factor (CTCF) at topologically associating domain (TAD) boundaries and also binds a subset of promoters/enhancers, was shown to be required for P-E looping (Kagey et al. 2010; El Khattabi et al. 2019), although acute depletion of cohesin has only limited effects on transcription (Rao et al. 2017). Weakened P-E communication was observed in several individual genes after knocking down the Mediator subunit MED12 (Kagey et al. 2010; Phillips-Cremins et al. 2013) or stripping away the Mediator complex from enhancers by knockdown of the activator ESRRB (Sun et al. 2019). However, P-E looping is only marginally affected after degradation of MED14, a subunit of Mediator that connects the HMT modules (El Khattabi et al. 2019; Jaeger et al. 2020). However, as Mediator has multiple subunits, it remains to be elucidated which subunit(s), if any, play critical roles in chromatin looping. In addition, a promoter may also interact with other *cis*-regulatory element such as enhancer-like promoters (Dao et al. 2017; Jung et al. 2019) and insulated neighborhood boundaries (Sun et al. 2019). The function of these interactions and how they are established are not understood.

It is largely unknown whether other components of transcriptional machinery such as TFIID participate in P-E interactions and other types of promoter-interacting chromatin looping. The TFIID subunit TAF3 binds both promoters and enhancers in mouse embryonic stem cells (mESCs) and displays functions similar to Mediator in maintaining pluripotency and mediating looping between promoters and enhancers (Liu et al. 2011). This suggests TFIID may be necessary for P-E contact. For a subset of genes, Pol II and other GTFs are found at enhancers in low amounts and at promoters in abundance (Koch et al. 2011), suggesting the PIC as a potential bridge for P-E contacts. Additionally, PICs at enhancers produce enhancer RNAs, which may stabilize P-E looping (Li et al. 2013; Hsieh et al. 2014). These facts suggest PICs may have a direct function in mediating P-E interactions. Genome-wide and loss-of-function studies using assays like promoter capture Hi-C and acute protein degradation are needed to determine whether the PIC plays a major role in establishing P-E or other chromatin loops.

Mediator and TFIID both contain multiple subunits. The minimal set of core Mediator subunits necessary for function within the PIC has been defined in yeast (Plaschka et al. 2015) and humans (Cevher et al. 2014). Additional activator-interacting subunits are required for P-E interactions and, for a given gene, could vary depending on the specific enhancer-bound activator(s). Previous studies indicate not all subunits are of equal importance in maintaining the functions of the complex (Kagey et al. 2010; Xu et al. 2018). Which subunits are essential for transcription and, perhaps, P-E interaction? What are the subunits that contribute to the possible collaboration between TFIID and Mediator? To answer these questions, we screened all TFIID/Mediator subunits by coupling RNA interference (RNAi) with messenger RNA sequencing (mRNA-seq). We identified TFIID and Mediator subunits whose depletion had substantial overlapping effects on the transcriptome. This analysis led to the identification of TAF12 and MED4 as key candidates to pursue further. Acute degradation using the auxin-inducible degron system (Natsume et al. 2016) revealed TAF12's important role in TFIID integrity and PIC assembly at promoters, and its role in Mediator binding at both promoters and enhancers. MED4 helps Pol II delivery to promoters but does not contribute to assembly of other PIC components. Through the use of promoter capture Hi-C, TAF12 was found to mildly contribute to promoter-interacting chromatin looping except for promoter–promoter interactions. In contrast, loss of MED4 globally decreases Pol II at enhancers and promoters but disrupts P-E looping for only a few genes.

Results

shRNA screen of TFIID and Mediator subunits

It is well documented that TFIID and Mediator are essential for gene expression, but a systematic investigation of the function of each individual subunit is rare. Studies have screened TFIID and Mediator subunits using RNAi for key factors in mESC state maintenance and acute myeloid leukemia (AML) progression (Kagey et al. 2010; Pijnappel et al. 2013; Xu et al. 2018). However, these screens relied mainly on morphology changes to identify

subunits of interest. It was unknown to what extent the transcriptome was affected in each knockdown (KD).

In our screen design, each TFIID/Mediator subunit was individually knocked down using an shRNA in mESCs (V6.5). Two or more shRNAs were designed and tested (Supplemental Fig. S1A), and the one with the strongest-fold KD was used in the screen. The KD was followed by mRNA-seq and a list of up-regulated or down-regulated (twofold cutoff) genes was identified by comparison with the control sample (Fig. 1A). mRNA-seq data reveal high specificity of each shRNA for its target gene (Supplemental Fig. S1B). Figure 1B summarizes the numbers of

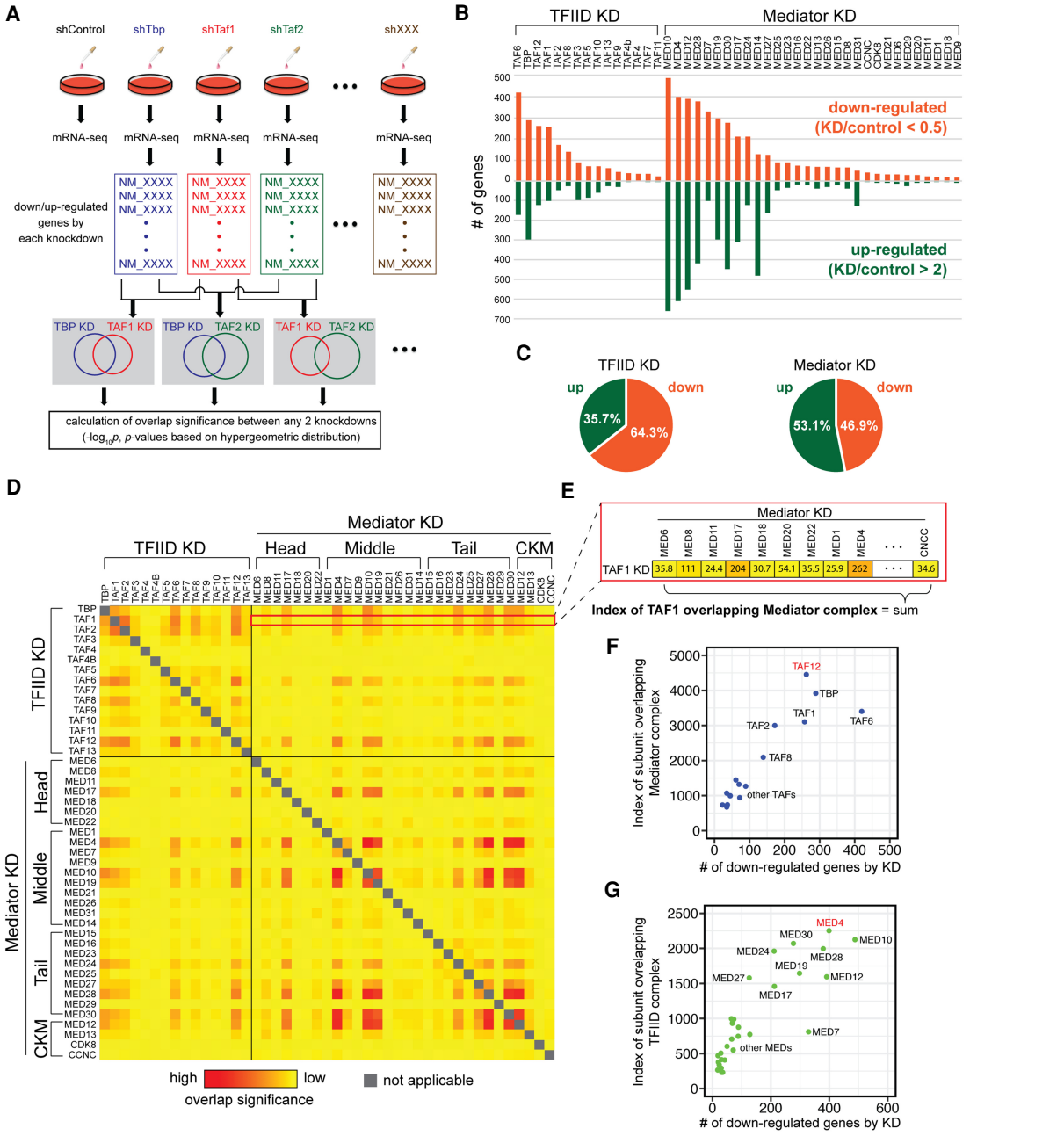

Figure 1. An shRNA screen identifies TAF12 and MED4 as key subunits of TFIID and Mediator. (*A*) Workflow of the shRNA screen. (*B*) Bar plots summarizing numbers of down-regulated and up-regulated genes in each KD. (*C*) Pie charts showing percentages of down-regulated and up-regulated genes. (*D*) Heat map showing the significance of all pairwise overlaps based on the down-regulated genes. (*E*) Enlargement of the row in the heat map in *D* showing overlap significance (numbers in grid) between down-regulated mRNAs in TAF1 KD and KDs of all Mediator subunits. The index of TAF1 overlapping Mediator complex is defined as the sum of these values. (*F*) Scatter plots showing each TFIID subunit's overlap index with the Mediator complex versus the number of down-regulated genes upon its KD. The *X*-axis indicates the number of down-regulated genes as in *B*. The *Y*-axis is the index of subunit overlap as in *E*. The subunit with the highest index is highlighted in red. (*G*) Same as *F* but plotting Mediator subunits.

genes down-regulated or up-regulated by each of the KDs. Two observations emerged from this analysis. First, different KDs impact the mESC transcriptome differently even for subunits in the same complex. For example, loss of MED10 down-regulates ~500 genes and up-regulates >600 while MED9 KD has a minimal effect despite similar KD levels (Supplemental Fig. S1A). This result suggests not all subunits contribute equally to transcription. Second, KDs lead to both down-regulation and up-regulation, although in the case of TFIID more genes are down-regulated, while in the case of Mediator similar numbers of genes are down-regulated or up-regulated (Fig. 1B,C; Supplemental Table S1). We believe the up-regulated genes are not due to some repressive function of Mediator or TFIID but are an indirect effect of differentiation caused by the KD, as we address later.

Although the KDs of some subunits dysregulate many genes, it is unclear whether distinct subunit KDs have a tendency to affect the same or distinct genes. We hypothesize that if two factors possess similar functions in transcription, genes impacted by KD of either factor will overlap in a statistically significant manner. To test this idea, we identified the intersection of all pairs of KDs for TFIID and Mediator and estimated their overlap significance based on a hypergeometric distribution (Fig. 1A). Figure 1D shows the significance of all pairwise overlaps calculated after intersecting the down-regulated genes (KD/control < 0.5). Several observations emerged from this analysis that agree well with previous structural or mass spectrometry studies. For example, cryo-EM analysis revealed that TAF1 and TAF2 recognize and bind DNA downstream from the TSS (Louder et al. 2016), in agreement with the strong transcriptomic overlap between their KDs ($P < 10^{-467}$). Cross-links are observed between MED10 and MED4 in Mediator (Plaschka et al. 2015). The KD of MED10 overlaps significantly with that of MED4 ($P < 10^{-848}$). These data support our hypothesis that the comparison of overlap indices can be used to identify subunits of TFIID and Mediator that affect similar genes by the same or complementary processes.

By summing the significance values of overlap between a specific TFIID subunit and all Mediator subunits, we defined the overlap index of this TFIID subunit with Mediator (example shown in Fig. 1E), or vice versa for a Mediator subunit overlapping the TFIID complex. Based on this index, TAF12 emerged as the strongest Mediator-overlapping TFIID subunit (Fig. 1F). Similarly, MED4 emerged as the strongest TFIID-overlapping Mediator subunit (Fig. 1G). We also estimated the significance of each pairwise overlap based on the intersection of up-regulated genes (KD/control > 2) (Supplemental Fig. S1C). Only weak overlaps were observed between TFIID and Mediator subunits, suggesting the two complexes collaborate mainly on gene up-regulation.

Acute degradation of TAF12 or MED4 down-regulates transcription

To better understand TAF12 and MED4 function, we used an auxin-inducible degron (AID) system (Fig. 2A,B) to create separate degron cell lines of both proteins (Natsume et al. 2016). Western blotting indicated successful knock-in of the *OsTir1* gene and fusion of mini-AID (mAID) tags to target proteins. Only a mild decrease of TAF12 and MED4 levels was observed after 30 min of auxin treatment, while substantial protein depletion was achieved after 6 h (Fig. 2C,D). We therefore chose a 6-h endpoint for all subsequent experiments because it is well within the 11.3-h doubling time of V6.5, and less likely to have indirect effects. The mAID does not alter the genome-wide binding profiles of either TAF12 or MED4 or the transcriptomes when comparing degron cell lines without auxin treatment with their parental wild-type (WT) mESCs (Supplemental Fig. S2A–F). These data suggest that mAID has little to no observable effect on the functions of TAF12 or MED4.

Because auxin-induced protein degradation occurs rapidly, we applied nascent or chromatin RNA-seq to more accurately quantify gene expression. Spike-in of human RNA was used for normalization between samples (see the Materials and Methods). TAF12 and MED4 depletion led to transcription down-regulation, although TAF12 degradation has a more dominant impact on the nascent transcriptome (Fig. 2E,F). The genes that decrease in the degron experiments cover most of the down-regulated genes from the shRNA screen (Supplemental Fig. S2G), demonstrating the reproducibility between direct protein depletion and KD in impairing transcription. Furthermore, a significant overlap is observed between the top 2000 impaired genes from the TAF12 and MED4 degrons (Fig. 2G), consistent with the shRNA screen. Gene ontology (GO) analysis indicates these overlapping genes are related to translation and gene expression (Fig. 2H).

Interestingly, after protein depletion using the AID system, only a small portion of the dysregulated genes (0.9% in TAF12 degron and 3.4% in MED4 degron) are up-regulated compared with those in the shRNA screen (31.9% in TAF12 KD and 60.4% in MED4 KD) (Supplemental Fig. S2H). This inconsistency suggests the up-regulated genes in the KD may be an indirect effect due to the long 72-h period of the shRNA experiments. Indeed, genes encoding master transcription factors (Nanog, Oct4, Esrrb, Klf4, Sall4, and Tbx3) are down-regulated upon TAF12 or MED4 loss (Fig. 2E), which previous studies suggest lead to cell differentiation (Kagey et al. 2010). GO analyses show that up-regulated genes in the shRNA screen are related to cell differentiation (Supplemental Fig. S2I). In sum, the data suggest that gene up-regulation in the TAF12 and MED4 KDs is likely caused by differentiation.

Acute degradation of TAF12 destroys TFIID and leads to loss of the PIC

TFIID contains two copies of TAF12, which lie in lobe A and lobe B, respectively (Fig. 3A; Patel et al. 2018). Coimmunoprecipitation (co-IP) experiments indicate that after TAF12 degradation, all tested TFIID subunits fail to coprecipitate with TAF1 as efficiently as in the control (Fig. 3B; Supplemental Fig. S3A). Strikingly, we also observed decreased levels of some TFIID subunits in the input

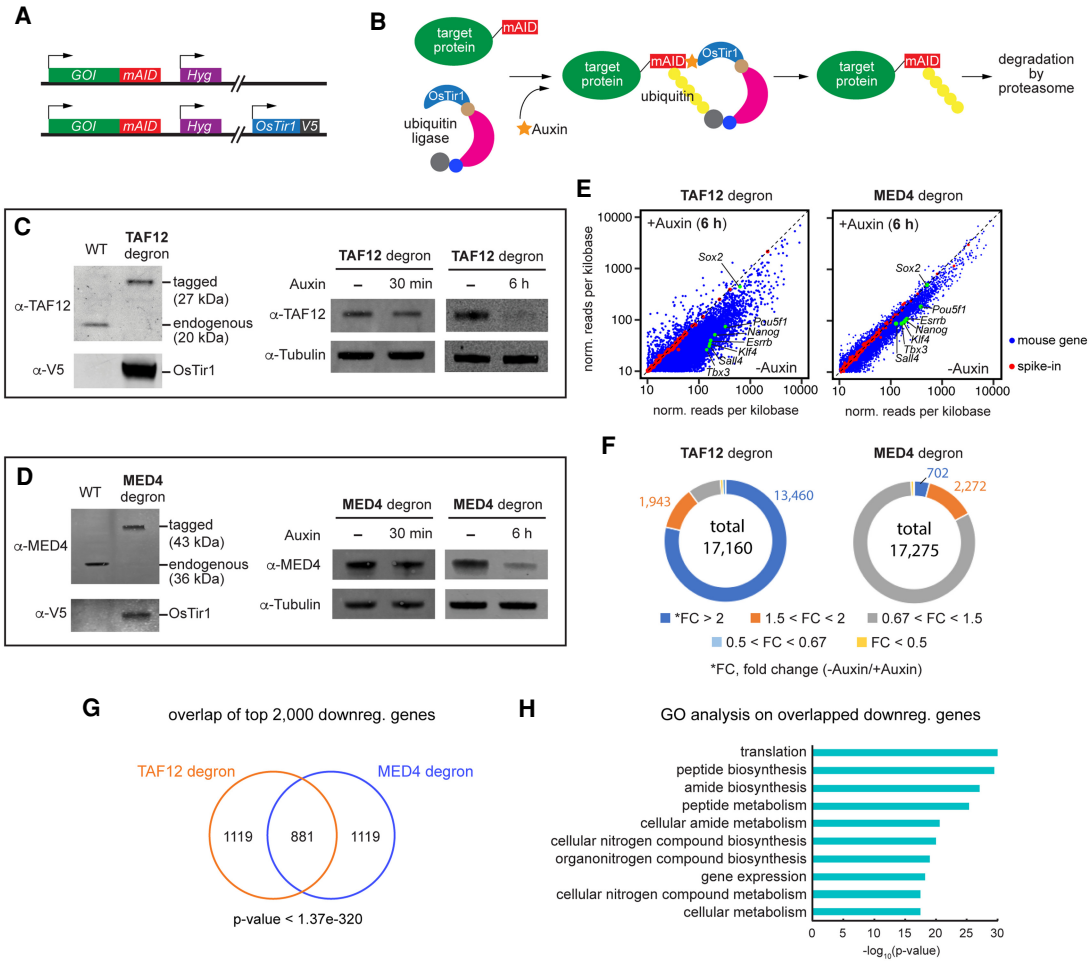

Figure 2. Acute degradation of TAF12 or MED4 down-regulates transcription genome-wide. (*A*) Schematic of genetic manipulation for the degron cell line. (GOI) Gene of interest, (Hyg) hygromycin-resistant gene. (*B*) Schematic of auxin-inducible protein degradation. (*C*, *left*) Western blotting comparing WT V6.5 with the TAF12 degron cell line. (*Right*) Western blotting showing degradation of TAF12 protein after 30-min and 6-h Auxin treatment in the degron cell line. (*D*) Same as *C* but showing MED4 degron cell line. (*E*) Scatter plots of nascent RNA levels of each gene in untreated (−Auxin) and treated (+Auxin) samples of TAF12 degron and MED4 degron. Spike-ins and pluripotency genes (*Nanog*, *Pou5f1*, *Sox2*, *Esrrb*, *Klf4*, *Tbx3*, and *Sall4*) are highlighted in red and green, respectively. (*F*) Donut charts showing numbers/proportions of genes classified by gene level changes upon auxin treatment. (*G*) Venn diagram showing the proportional overlap of the top 2000 genes down-regulated upon TAF12 and MED4 degradation. The *P*-value was calculated based on a hypergeometric distribution. (*H*) Gene ontology analysis of the overlapping genes in *G*.

samples. We did not expect this result because TAF12 is of low molecular weight (~20 kDa) and TAF12 locates to the surface and not to the cores of lobes A and B (Fig. 3A). Chromatin immunoprecipitation followed by sequencing (ChIP-seq) confirmed the loss of TFIID binding at promoters in vivo (Fig. 3C,D). Interestingly, recruitment of TBP to promoters is only mildly affected. Nevertheless, these data indicate TAF12 is a cornerstone of TFIID integrity.

TAF12 is shared by TFIID and another protein complex termed SAGA (Spt-Ada-Gcn5-acetyltransferase). SAGA is a coactivator that regulates transcription by modifying histones through its GCN5 and USP22 subunits. We were unable to chromatin-immunoprecipitate GCN5 similar to what others have reported (Hirsch et al. 2015). However, ChIP-seq of H3K9ac, catalyzed by GCN5, reveals only small changes at promoters (Fig. 3C,D), suggesting that depletion of TAF12 has little effect on SAGA's HAT activity. We also knocked down *Gcn5* and *Usp22* by shRNA in mESCs followed by mRNA-seq and integrated these data with those of the shRNA screen (Supplemental Fig. S3C,D). GCN5 or USP22 KD has much weaker effects on the transcriptome compared with TAF12 or MED4 KD (Supplemental Fig. S3E). Importantly, no dominant overlap is observed between SAGA and TAF12 or MED4 KDs when comparing down-regulated genes (Supplemental Fig. S3F). SAGA is also capable of delivering TBP to promoters (Papai et al. 2020). However, TBP binding is barely affected upon TAF12 degradation (Fig. 3C,D), suggesting this function of SAGA is not impacted. These observations support the idea that transcription down-regulation after TAF12 degradation is caused mainly by loss of TFIID and not defects in SAGA's

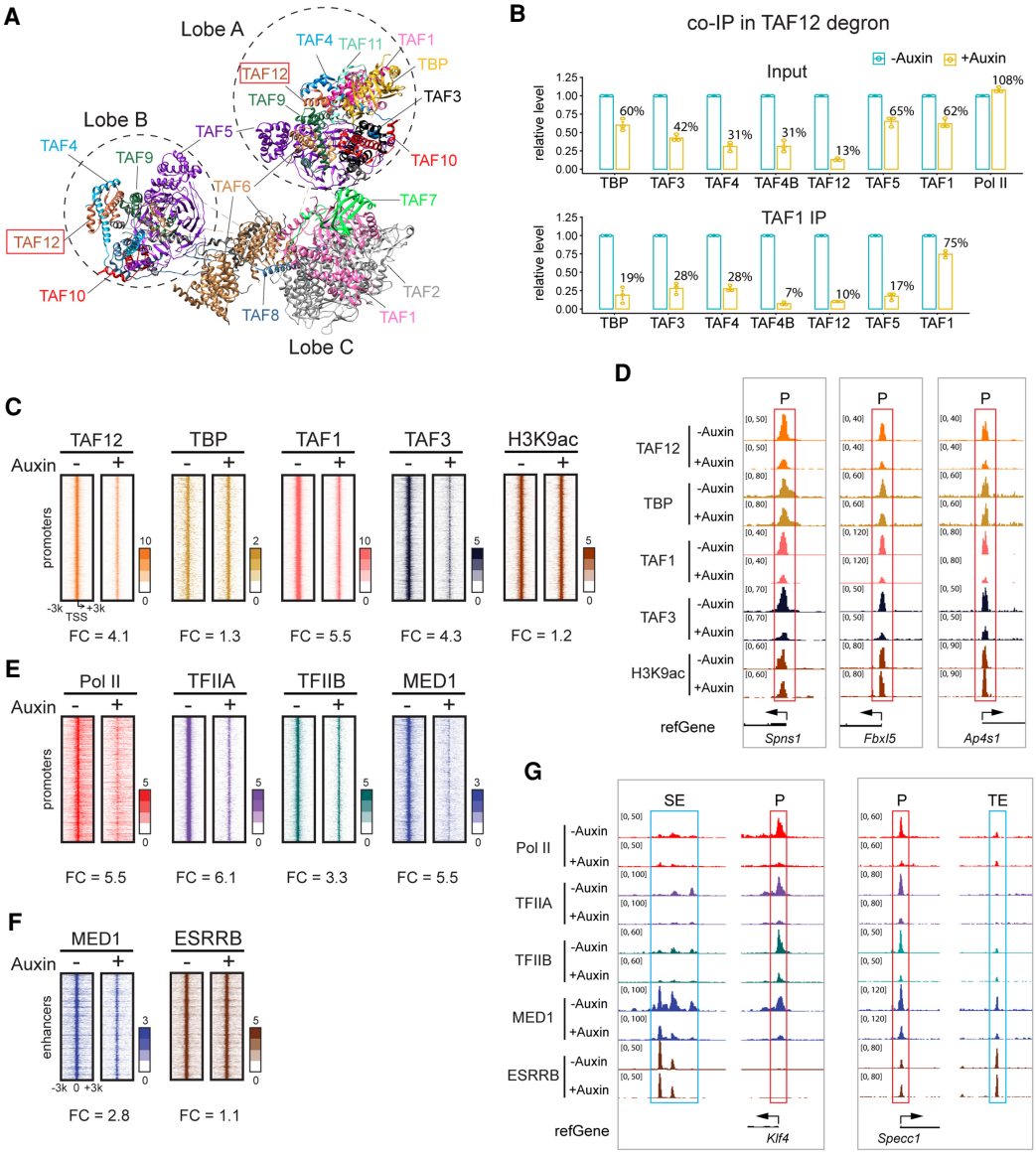

Figure 3. TAF12 degradation destroys TFIID and leads to loss of the PIC. (*A*) Cryo-EM structure of the TFIID complex (PDB: 6MZL) (Patel et al. 2018). The two copies of TAF12 are highlighted in the red boxes. (*B*) Relative protein levels in the input and TAF1 IP samples of the co-IP experiments in TAF12 degron cells comparing auxin-treated (+Auxin) with untreated (−Auxin). Protein levels in the untreated samples were normalized to 1. Relative levels of the treated samples are shown as percentages. Bar graphs and the percentages show the average of three replicates. (*C*) Heat maps showing binding of TFIID subunits TAF12, TBP, TAF1, and TAF3 along with H3K9ac at promoters in untreated and auxin-treated TAF12 degron cells. Color scales indicate significance ($-\log_{10}P$). (FC) Fold change decrease of −Auxin/+Auxin. (*D*) Browser tracks of examples showing TAF12, TBP, TAF1, TAF3, and H3K9ac binding at promoters (highlighted in the red boxes) in untreated and auxin-treated TAF12 degron cells. The *Y*-axis indicates normalized counts. (P) Promoter. (*E*) Heat maps showing binding of other PIC components including Pol II, TFIIA, TFIIB, and MED1 at promoters in untreated and auxin-treated TAF12 degron cells. (*F*) Heat maps showing binding of MED1 and ESRRB at enhancers in untreated and auxin-treated TAF12 degron cells. (*G*) Browser tracks of examples showing Pol II, TFIIA, TFIIB, MED1, and ESRRB binding at promoters (red boxes) and enhancers (blue boxes). (P) Promoter, (SE) superenhancer, (TE) typical enhancer.

histone acetylation/deubiquitylation or TBP loading activities. However, we cannot completely rule out the possibility that SAGA may be impacted by TAF12 depletion in an unknown manner, which may affect some observations in our study.

The loss of TFIID dramatically impacts the genome-wide binding of other PIC components at promoters including Pol II, TFIIA, and TFIIB (Fig. 3E,G), confirming the fundamental role of TFIID in PIC assembly. Mediator regulates transcription in collaboration with the PIC, but it is unknown whether recruitment of Mediator complex at promoters is PIC-dependent in vivo. ChIP-seq reveals Mediator is lost at promoters in parallel with the loss of the PIC (Fig. 3E,G). Unlike TFIID, Mediator binds both

promoters and enhancers. Surprisingly, although there is little TAF12 enrichment at enhancers (Supplemental Fig. S3B), Mediator binding there is weakened by TAF12 degradation (Fig. 3F,G). Mediator is recruited to enhancers by transcription factors such as ESRRB (Sun et al. 2019). One possible explanation is that TAF12 degradation affects binding patterns of ESRRB, which in turn removes Mediator from enhancers. However, ESRRB binding is not altered (Fig. 3F,G), suggesting lessened Mediator binding at enhancers is not caused by loss of this transcription factor. These effects are similar for superenhancers (SEs) and typical enhancers (TEs) (Supplemental Fig. S3G,H). In sum, these results suggest that TFIID is fundamental to PIC assembly at promoters. Moreover, the intact PIC supports Mediator recruitment to promoters and enhancers. In turn, the result implies that the amount of Mediator at enhancers is not solely a function of activators but is dependent on the presence of a PIC. Because Pol II binds the Mediator, it raises the question of what drives Pol II levels at the PIC.

MED4 depletion impairs Pol II binding at promoters but has no effects on other PIC components

MED4 is a subunit within the middle module of Mediator (Fig. 4A). Co-IP experiments show that MED4 degradation leads to >50% decreases of MED1 and MED9, while the rest of the tested Mediator subunits are largely retained in the complex (Fig. 4B; Supplemental Fig. S4). The decreased abundance of MED1 and MED9 is consistent with cryo-EM structural studies, where MED1 and MED9 interact with MED4 (Abdella et al. 2021; Zhao et al. 2021). Similarly, in vivo, MED4 loss results in decreased binding of MED1, but not MED6, at promoters and enhancers (Fig. 4C,D). MED6 lies within the head module of Mediator (Fig. 4A) and would be predicted to bind only if this module is largely intact after MED4 depletion.

A key function of Mediator in regulating transcription is to promote PIC assembly through specific interactions between Mediator subunits and different PIC components (Soutourina 2018). In yeast, the MED4–MED9 interaction with the Pol II foot domain in the RPB1 subunit is one of four points of contact observed between Mediator and Pol II (Tsai et al. 2017). In humans, the Mediator plank domain contacts RPB8 instead of RPB1 (Abdella et al. 2021). Co-IP of Mediator indicates a consistent 50% reduction in the amount of bound Pol II upon MED4 degradation (Fig. 4B; Supplemental Fig. S4). In agreement with this result, ChIP-seq data reveal Pol II binding at promoters decreases by twofold upon MED4 depletion. In contrast, TFIIA, TFIIB, TFIID (TAF1), and TFIIH (XPB) are mainly unaffected (Fig. 4E,F). These data indicate that MED4 functions in recruiting Pol II to promoters but does not influence the overall genome-wide level of other PIC components.

PIC and MED4 have minimal effects on promoter-interacting chromatin looping

Promoters interact with different *cis*-regulatory elements through chromatin looping. To obtain a global view of how promoters interact with different types of genomic loci (e.g. promoters or enhancers) across the genome, we applied promoter capture Hi-C (PCHi-C), which uses biotinylated RNA probes to capture chromatin interactions associated with promoters from a Hi-C library (Fig. 5A). Histone modifications can be used to identify distinct genomic regions including promoters, enhancers, transcribed regions, and repressed regions. Based on the histone modification status, a ChromHMM (chromatin state analysis) model (Chronis et al. 2017) was used to divide the mESC genome into 18 different types of regions or "chromatin states" (Fig. 5B, see the legend for the full name of each state). We investigated how likely it was that a particular chromatin state interacts with promoters genome-wide by combining PCHi-C data and the ChromHMM model. Using the CHiCAGO (capture Hi-C analysis of genomic organization) analysis platform (Cairns et al. 2016), significant loops (P-value $<10^{-5}$) were identified from PCHi-C. Each significant loop bridges the interaction between a probed promoter and a promoter-interacting region (PIR), which may be located in any of the 18 different chromatin states. We calculated the percentages of PIRs located in different chromatin states (Supplemental Fig. S5A) and the percentage of each chromatin state's size occupancy in the genome (Supplemental Fig. S5B). Based on these percentages, the fold enrichment of PIRs in each chromatin state was calculated (Supplemental Fig. S5C). Consistent with the fact that promoters frequently interact with enhancers and other promoters (Dao et al. 2017; Jung et al. 2019), PIRs are most enriched in active promoters (1_PromA; 10.8-fold), followed by poised promoters (2_PromP; 6.2-fold) and acetylated enhancers (3_EnhA; fivefold). Interestingly, enrichment is also observed for other chromatin states such as transcribed and polycomb regions, suggesting these regions may also possess regulatory activities.

We next investigated the effects of TAF12 or MED4 degradation on promoter-interacting chromatin looping. Because PCHi-C data are typically not saturating, we applied stringent cutoffs to filter out genes and interactions that had fewer PCHi-C counts or lower significance (see the Materials and Methods). Although this approach lowers the sample sizes, it generates more reliable analyses. Based on the 18 chromatin states, all promoter-interacting chromatin loops are classified into six groups comprising loops of promoter–promoter (P-P), promoter–enhancer (P-E), promoter–transcribed region (P-T), promoter–polycomb region (P-PC), promoter–heterochromatin (P-Het), and promoter–low signal region (P-L). Figure 5C shows how different types of promoter-interacting loops change after TAF12 degradation. As indicated in Figure 3, TAF12 degradation leads to a large decrease in PICs and a dominant decrease in Mediator bound to enhancers. Thus, the effects on looping could be a consequence of any of these effects. The box plots illustrate the $\log_2$ ratio of normalized PCHi-C counts in the presence versus the absence of a 6-h auxin treatment. Analysis of group 1 in Figure 5C indicates interaction between a promoter and another active promoter is largely unaffected, according to the median value. However, a subtle decrease is

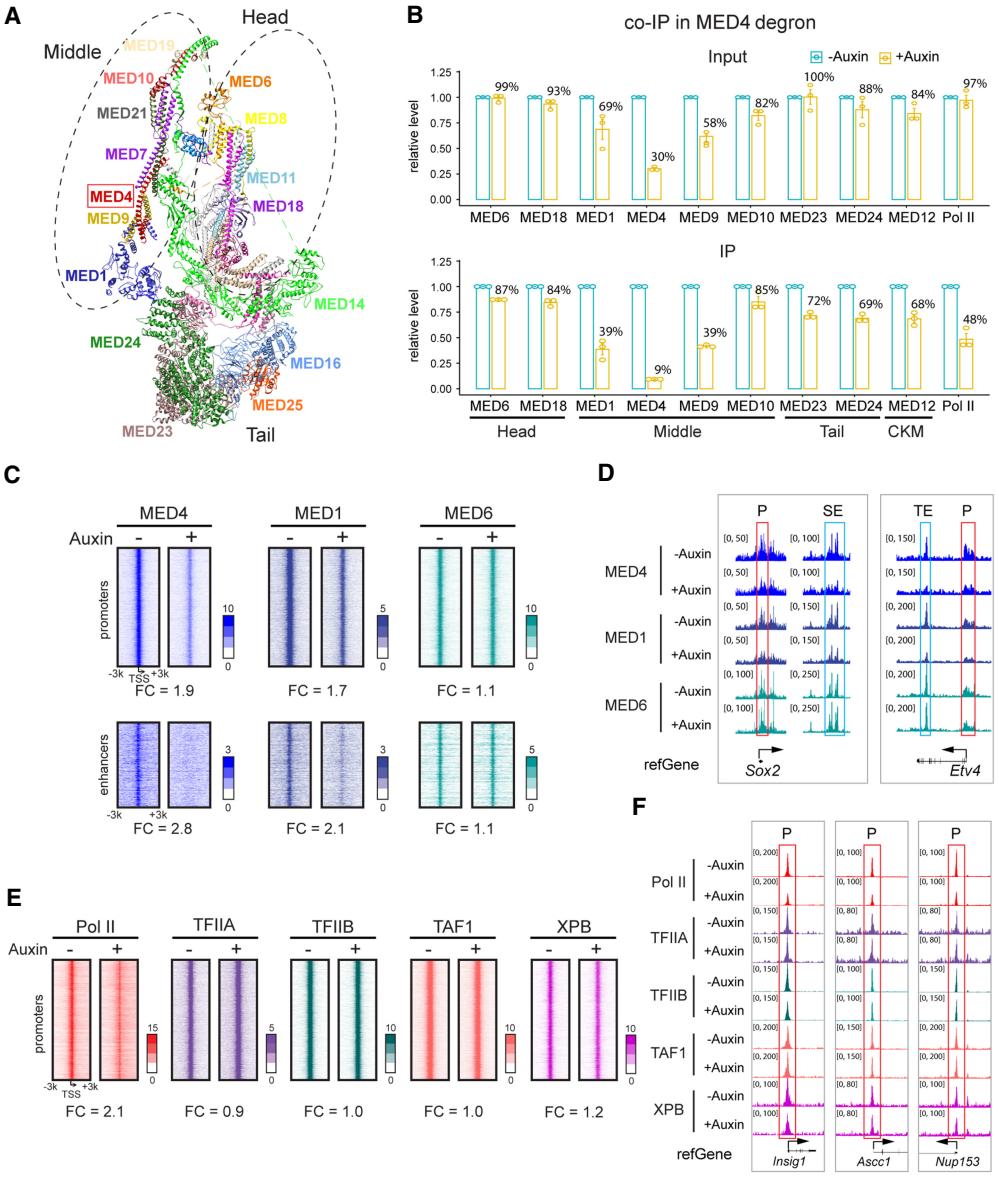

Figure 4. MED4 degradation impairs Pol II binding but has little effect on assembly of other PIC components measured. (*A*) Cryo-EM structure of the Mediator complex (PDB: 6W1S) (Zhao et al. 2021). MED4 is highlighted in the red box. (*B*) Relative protein levels in the input and IP samples of the co-IP experiments in MED4 degron cells comparing auxin-treated (+Auxin) with untreated (−Auxin). The protein level in the untreated sample was normalized to 1. Relative levels of the treated samples are shown as percentages. Bar graphs and the percentages show the average of three replicates. (*C*) Heat maps showing binding of Mediator subunits MED4, MED1, and MED6 at both promoters and enhancers in untreated and treated MED4 degron cells. Color scales indicate significance ($-\log_{10}P$). (FC) Fold change of −Auxin/+Auxin. (*D*) Browser tracks of examples showing MED4, MED1, and MED6 binding at promoters and enhancers. The *Y*-axis indicates normalized counts. (P) Promoter, (SE) superenhancer, (TE) typical enhancer. (*E*) Heat maps showing binding of other PIC components Pol II, TFIIA, TFIIB, TAF1, and XPB (TFIIH) at promoters in untreated and auxin-treated MED4 degron cells. (*F*) Browser tracks of examples showing Pol II, TFIIA, TFIIB, TAF1, and XPB binding at promoters. (P) Promoter.

observed for other chromatin states, although the change is much less than twofold, and far less than the approximately fivefold depletion of PICs. These data suggest that in the absence of PICs after TAF12 depletion, promoters associate slightly less well with many chromatin states but still fully associate with other active promoters.

Next we performed the same analysis on PCHi-C data from the MED4 degron. The box plots reveal no dominant effects of MED4 depletion on most types of promoter-interacting chromatin loops (Fig. 5D). This reveals that although MED4 plays a key role in recruiting Pol II to promoters (Fig. 4), it does not broadly influence promoter-associated chromatin looping including P-E interactions. We also performed this analysis using a different enhancer annotation file from Whyte et al. (2013) in which superenhancers (SEs) and typical enhancers (TE) are distinguished.

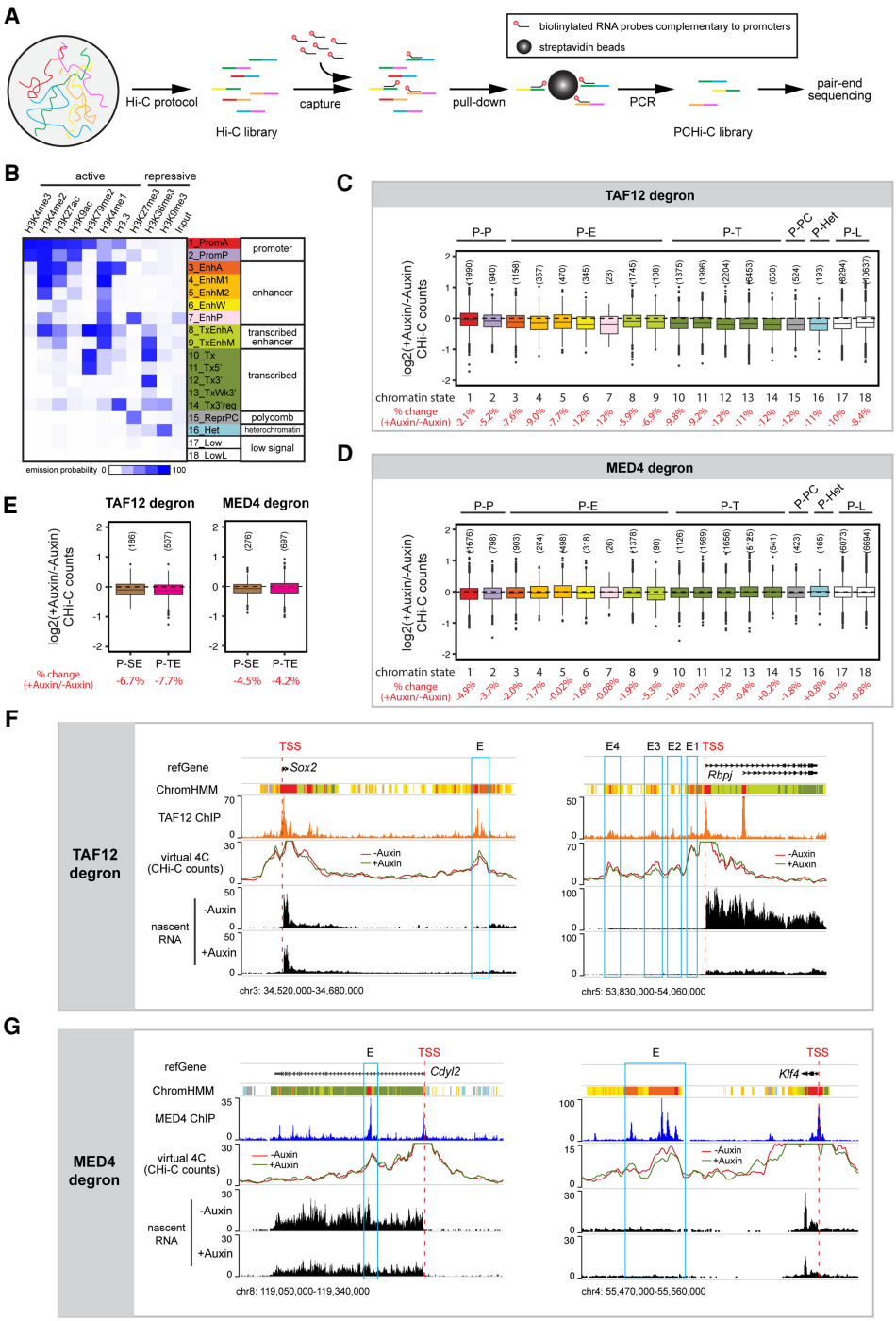

Figure 5. TAF12 and MED4 have minimal effects on promoter-interacting chromatin loops. (*A*) Workflow of promoter capture Hi-C. (*B*) Frequency of each histone mark, H3.3, and input signal of an 18-state ChromHMM analysis. (PromA) Active promoter, (PromP) poised promoter, (EnhA) acetylated enhancer, (EnhM1) moderately acetylated enhancer type 1, (EnhM2) moderately acetylated enhancer type 2, (EnhW) weakly acetylated enhancer, (EnhP) poised enhancer, (TxEnhA) transcribed acetylated enhancer, (TxEnhM) transcribed moderately acetylated enhancer, (Tx) strong transcription, (Tx5′) transcribed 5′ preferential, (Tx3′) transcribed 3′ preferential, (TxWk3′) weakly transcribed 3′preferential, (Tx3′reg) transcribed and regulatory 3′ preferential, (ReprPC) polycomb, (Het) heterochromatin, (Low) low state, (LowL) lower low state. (*C*) Box plots showing changes of different types of promoter-interacting chromatin loops upon loss of TAF12. The *Y*-axis is the $\log_2$ ratio of the normalized PCHi-C counts in treated versus untreated samples. The *X*-axis indicates the 18 different chromatin states. Each box indicates the median and interquartile range. The percentage change *below* each box is based on the median. Color and number codes in the boxes are as in *B*. Sample size of each chromatin state is indicated by the number in the brackets. (P-P) Promoter–promoter loop, (P-E) promoter–enhancer loop, (P-T) promoter–transcribed region loop, (P-PC) promoter–polycomb loop, (P-Het) promoter–heterochromatin loop, (P-L) promoter–low signal region loop. (*D*) Same as *C* but plotting data upon loss of MED4. (*E*) Box plots showing changes of promoter–superenhancer (P-SE) and promoter–typical enhancer (P-TE) looping upon loss of TAF12 or MED4. (*F*,*G*) Browser tracks of examples showing the impact of TAF12 (*F*) or MED4 (*G*) degradation on promoter–enhancer looping. Data of ChromHMM, TAF12/MED4 ChIP-seq, virtual 4C, and nascent RNA-seq are shown.

Again, neither TAF12 nor MED4 depletion disrupts P-SE or P-TE looping (Fig. 5E).

We focused on individual genes to illustrate both the major trends and the interesting exceptions. 4C (circularized chromosome conformation capture) is a method for studying how a genomic locus (e.g., a promoter) interacts with other loci across the genome. To better visualize PCHi-C for an individual gene, we extracted data associated only with this gene and PCHi-C counts were normalized between samples and plotted on the browser tracks (virtual 4C) (see the Materials and Methods). Figure 5F illustrates the *Sox2* gene, which is a good example showing how a P-E interaction is unaffected upon TAF12 degradation. In a different example, the *Rbpj* promoter interacts with four enhancers. Looping to three of them is unchanged while the other one is only slightly decreased. In Figure 5G, MED4 degradation does not impact P-E looping for *Cdyl2* and only weakly down-regulates the P-SE interaction of *Klf4*. Additional examples showing interesting exceptions are in Supplemental Figure S5, D and E. TAF12 depletion weakens a P-T interaction in *PPil4* and *Stn1*, indicating the PIC may contribute to promoter interactions with transcribed regions for these genes. P-E interactions are also down-regulated in *Stn1* as well as *Nanog*, which encodes a master transcription factor critical for mESC pluripotency (Supplemental Fig. S5D). Upon MED4 degradation, P-E and P-P looping are weakened in different genes (Supplemental Fig. S5E). Our previous study shows P-E interaction of *Tbx3* is weakened after Mediator depletion from its superenhancer proxied by ESRRB KD (Sun et al. 2019). Interestingly, the same P-E contact is also dominantly down-regulated upon loss of MED4 (Supplemental Fig. S5E). This suggests MED4 regulates the bridging of some, but not all, P-E contacts.

Discussion

Our shRNA screen identified key TFIID/Mediator subunits in genome-wide transcription. Based on the overlap index and number of down-regulated genes, we chose to pursue TAF12 and MED4 to determine whether they had similar or complementing roles in P-E communication. Auxin-inducible degrons were constructed and found to impair TFIID and Mediator in specific ways for loss-of-function studies. As shown in the schematic in Figure 6, degradation of TAF12 led to drastic loss of both intact TFIID and PICs. Degradation of MED4 led to an ~50% reduction in the amount of Pol II associated with Mediator, while other Mediator subunit associations were only mildly affected (i.e., <25%), except for MED1 and MED9 at the end of the Mediator Plank subdomain, which decreased by ~60%. Neither TAF12 nor MED4 degradation drastically disrupts P-E looping. Here, we first discuss TAF12 and MED4 function in the coactivator complexes, and then their possible roles in chromatin looping.

Correlation of TAF12 with TFIID and PIC

TAF12 is present within the A and B lobes of TFIID. Degradation of TAF12 led to a reduction of intact TFIID as measured using co-IP by TAF1 in lobes A and C. Loss of TAF12 also drives degradation of other TFIID subunits, which is also observed in AML and *Drosophila* cells (Wright et al. 2006; Xu et al. 2018). This degradation in turn led to decreased binding of TFIID at promoters and a dominant reduction in PIC assembly as measured by ChIP-seq of key components including TFIIA, TFIIB, Pol II, and Mediator. The loss of PIC assembly correlated with a dramatic decrease in nascent transcription genome-wide. Interestingly, although TFIID is destroyed upon TAF12 degradation, TBP binding to promoters is only weakly affected. This observation seems inconsistent with the model in which TBP binding to the promoter is dependent on TAFs (Patel et al. 2018). SAGA is also capable of TBP delivery to promoters (Papai et al. 2020). Thus, TBP binding at promoters may be mediated by SAGA after TAF12 degradation. Either way, TBP binding alone does not appear to support PIC assembly.

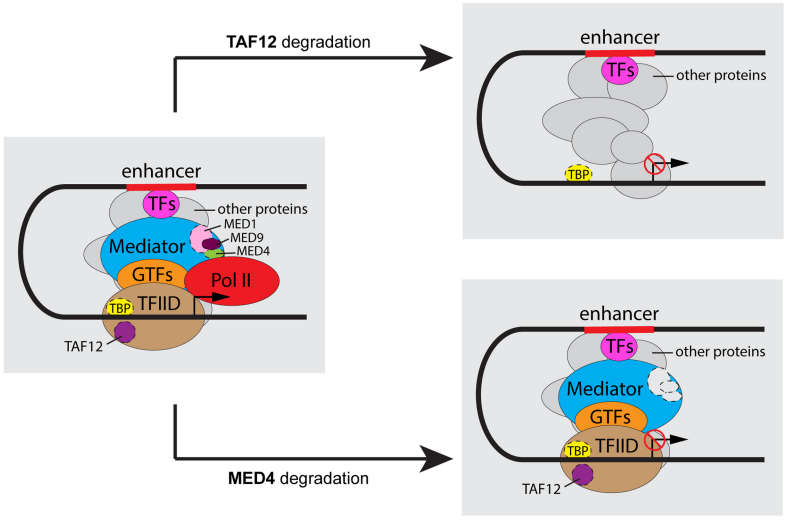

Figure 6. Schematic showing how TAF12 or MED4 degradation affects PIC binding and promoter–enhancer looping.

Although TAF12 is shared with the SAGA complex, loss of TAF12 barely affects the level of GCN5-catalyzed H3K9 acetylation. Knockdown of GCN5 and another key subunit, USP22, had limited effects on transcription in mESCs and revealed little overlap of down-regulated genes with those of TAF12 KD. This result is consistent with a previous report showing *Gcn5*-null mESCs grow well and result in no global failure in transcription (Lin et al. 2007). In addition, our group has shown that SAGA does not contribute to PIC assembly and stimulates, but is not necessary for, chromatin transcription in vitro in mammalian nuclear extracts (Chen et al. 2012). Although SAGA and TFIID appear to be needed globally for transcription in yeast (Baptista et al. 2017; Donczew et al. 2020), our studies suggest that in mESCs, SAGA subunits GCN5 and USP22 are not essential for genome-wide transcription.

Importantly, loss of the PIC leads to a decrease of Mediator binding to enhancers genome-wide. We previously showed that Mediator binds directly to the transcription factor ESRRB. Depletion of ESRRB leads to reductions in Mediator at enhancers, specifically at bound ESRRB sites (Sun et al. 2019). Importantly, Mediator was lost at ESRRB sites in the TAF12 degron even though the binding of ESRRB remained unchanged. This result suggests that despite its direct interaction with a well-studied TF, the PIC was necessary for efficient Mediator binding to enhancers and promoters bound by ESRRB. This observation in turn suggests that the PIC influences Mediator levels likely through direct interactions. In yeast, loss of TFIID also decreases binding of Mediator to the UASs (Grünberg et al. 2016), reinforcing the idea that PIC functions cooperatively with the enhancer as opposed to independent binding events.

Correlation of MED4 with Mediator and Pol II

Mediator is known to bind to enhancers and promoters. Mediator's association with Pol II has led to the hypothesis that it delivers Pol II to promoters, but there has been little functional evidence to support this hypothesis. Loss of Mediator has been shown to influence Pol II levels at promoters, but it has not been clear whether this is due to other functions conferred by Mediator on the PIC or loss of Pol II associated with Mediator. Here we found that depletion of MED4 decreases Pol II binding at promoters by twofold genome-wide while leaving Mediator binding to enhancers and promoters largely intact except for MED1 and MED9, which are attached to the plank domain along with MED4 (Fig. 4). This observation strongly implies that Mediator delivers Pol II to the PIC. Loss of MED4 has little effect on TFIIB binding, suggesting that the TFIIB interaction with Pol II is dependent on Mediator. As such, the Mediator–Pol II interactions could be viewed as a rate-limiting step in the transcription of the gene.

Promoter-associated chromatin looping and PIC/Mediator

PCHi-C integrated with ChromHMM data reveal promoters interact with different types of loci including promoters, enhancers, transcribed regions, and even repressed regions within heterochromatin or bound by polycomb. P-E looping has been extensively studied, but it is unclear whether the PIC contributes to the establishment of P-E communication. A previous study shows the PIC is likely dispensable for the interaction between the locus control region and the proximal promoter of β^{maj} globin gene in mouse erythroid leukemia cells because the loop is maintained after deletion of the core promoter (Krivega and Dean 2017). Our studies indicate the loss of PICs upon loss of TAF12 leads to only a mild decrease of P-E looping, inconsistent with the dramatic decrease in transcription. It is worth noting that Mediator binding is impaired at both promoters and enhancers upon TAF12 degradation. Thus, our study supports the idea that Mediator is not an essential player in maintaining global P-E interactions, consistent with previous reports (El Khattabi et al. 2019; Jaeger et al. 2020). Recent studies reveal P-P interactions are also important for gene activation (Dao et al. 2017; Jung et al. 2019). However, although the PIC binds all active promoters, PIC disassembly has no effect on the communication between two active promoters. The slight difference between the PIC's effects on P-P and P-E loops may suggest P-P and P-E loops are established by different mechanisms.

We found MED4 degradation impairs Pol II binding and global transcription but has no effect on any classified types of promoter-interacting chromatin loops. This result is consistent with a recent study showing that rapid degradation of Pol II does not affect genome organization in mESCs (Jiang et al. 2020). This observation also supports that Mediator is not essential for global P-E looping. However, exceptions were found in our studies, such as *Tbx3*. The interaction between the *Tbx3* promoter and its superenhancer is sensitive to MED4 degradation, as shown in this study, and loss of Mediator by ESRRB KD (Sun et al. 2019). On the other hand, TAF12 degradation does not destroy the *Sox2* promoter's interaction with its superenhancer. Interestingly, CTCF and cohesin bind both the *Sox2* promoter and the superenhancer (Zhou et al. 2014). CTCF/cohesin may participate in the *Sox2* P-E interaction, thus buffering the gene and its expression from loss of the PIC and Mediator. These facts also reveal the complexity of P-E or other chromatin looping events. Although we observed very clear evidence for P-E looping, it appeared that only a small subset of enhancers is sensitive to PIC or MED4 degradation. Perhaps there is a balance of productive looping mediated by the coactivators and unproductive looping controlled by other factors. Distinguishing these two types of looping will require further investigation.

Application of the shRNA screen

Unlike many multisubunit protein complexes, TFIID and Mediator HTM have no catalytic activities; thus, there is no apparent "key subunit." Although cryo-EM structures can help find the central core subunit that forms an interface important for assembly of other subunits (e.g., MED14 in Mediator), functional studies are still necessary

to elucidate each subunit's function. Strikingly, in our shRNA screen, MED14 KD does not result in significant gene down-regulation (Fig. 1B), in contrast to two studies in mouse lymphoma cells and human cancer cells (El Khattabi et al. 2019; Jaeger et al. 2020). It has been reported that MED14-defective zebrafish embryos do not display global defects in transcription (Burrows et al. 2015). This observation is consistent with our MED14 KD data and may indicate that MED14 is not required for global transcription in embryos/mESCs, although further studies are needed to prove it.

Our shRNA screen identified key TFIID/Mediator subunits whose KD can be used to abrogate the complex for loss-of-function studies. Indeed, TAF12 degradation destroys TFIID. These "key subunits" may be potential therapeutic targets in cancer. In agreement with this idea, knockdown of TAF12 was reported to suppress AML (Xu et al. 2018). Thus, our shRNA screen not only illustrates the importance of each TFIID/Mediator subunit but also provides a resource for finding targets in loss-of-function studies and cancer therapy. Our shRNA screen also has limitations. Knockdown of a subunit could have a minimal effect on transcription not because it does not contribute, but because enough of this subunit remains to support function.

Materials and methods

Cell culture

Wild-type V6.5 and degron cell lines were grown as described (Sun et al. 2019).

Antibodies

Antibodies used for immunoblotting, co-IP, and ChIP-seq are listed in Supplemental Table S2.

shRNA plasmid construction

Sequences of shRNA targeting different genes were designed with Invitrogen's BLOCK-iT RNAi designer (https://rnaidesigner.thermofisher.com/rnaiexpress) and placed into pSuper.puro (Oligoengine). Two to five different sequences were designed for each gene. These are listed in Supplemental Table S3.

shRNA plasmid transfection

MEF-depleted V6.5 cells were grown to ~50% confluency in 12-well plates before being transfected with 1.8 µg of shRNA plasmids using Lipofectamine 2000 following the manufacturer's instructions. Twenty-four hours after transfection, 1 µg/mL puromycin was added and cells were selected for 72 h before downstream analysis.

qPCR

Total RNA was extracted with TRIzol reagent following the manufacturer's instructions and analyzed by real-time qPCR using FastStart SYBR Green master mix (Roche) on a Mx3000P multiplex quantitative PCR system (Stratagene). Results from three replicates were normalized to *Gapdh*. Primers are in Supplemental Table S4.

Degron cell line construction

To construct a cell line bearing V5-tagged OsTir1, V6.5 was transfected with pEN396 and pX330-EN1201 plasmids (Nora et al. 2017) using Lipofectamine 2000. After 6 h, cells were passed into a dish with DR4 MEF feeders. After 2 d, 1 µg /mL puromycin was added and resistant colonies were picked, expanded, and verified by PCR. Construction of TAF12 or MED4 degron cell lines used CRISPR as described (Natsume et al. 2016). Guide RNA sequences, primers for amplification, and genotyping are listed in Supplemental Table S5.

Nuclear extraction

Nuclear extracts were prepared as described (Dignam et al. 1983).

Coimmunoprecipitation

Two milligrams of nuclear extract was incubated overnight at 4° C in 450 µL of PBS with 2–5 µg of antibody or IgG, captured on Dynabeads Protein A/G, washed, and eluted with 1× SDS loading buffer.

RNA-seq

mRNA-seq was done as previously described (Sun et al. 2019). Nascent RNA-seq was performed as described using 500,000 human BEAS-2B cells as a spike-in mixed with 10 million mESCs. Fractionation, RNA extraction, library construction, and sequencing were as described (Sun et al. 2019).

ChIP-seq

ChIP-seq was performed as described (Sun et al. 2019).

Promoter capture Hi-C

In situ Hi-C was as described (Rao et al. 2014). SureSelect adaptor (Agilent) was added to DNA ends following the manufacturer's protocol, and amplified with six to eight PCR cycles. PCR products were purified and concentrated. Seven-hundred-fifty nanograms was hybridized to custom biotinylated RNA probes as described by Agilent, and captured by Dynabeads MyOne Streptavidin T1 beads. The captured DNA was amplified on the beads using Agilent's indexing primers. The library was purified and sequenced on NovaSeq 6000 S4. All RNA-seq, ChIP-seq, and promoter capture Hi-C experiments were performed with two biological replicates. Pearson's correlation coefficients between replicates are listed in Supplemental Table S6.

Sequencing data analysis

mRNA-seq reads were mapped to mm9 and normalized to RPKM as previously described (Sun et al. 2019). For nascent RNA, sequence reads within the entire gene body were counted using a custom script. An RPK (reads per kilobase) value was calculated by dividing read counts by gene body size. Reads derived from human cell spike-ins were counted by mapping reads to hg38. RPK values were normalized to the spike-ins. ChIP-seq data were analyzed as described (Sun et al. 2019).

Promoter capture Hi-C sequence reads were processed by HiCUP (Wingett et al. 2015) with default options for mapping,

pairing, filtering, and deduplication. The unique and valid read pairs were further processed by CHiCAGO (Cairns et al. 2016). A chinput file was generated containing raw counts for each interaction. Loops were called with settings for four-cutter restriction enzyme digestion as suggested (https://bitbucket.org/chicagoTeam/chicago/src/master). A CHiCAGO score >5 was used as the cutoff for significant loops. For analyses in Figure 5, C–E, a loop was taken into consideration only when (1) the length of the loop was >10 kb, (2) the loop was significant in either the auxin-treated or untreated sample, (3) the bait promoter associated with this loop had >3000 usable PCHi-C counts identified for the bait promoter (i.e., *cis*-pairs interacting >10 kb), and (4) PCHi-C counts were >50 in either sample. A loop was assigned to a chromatin state when this chromatin state had a minimum 1-bp overlap with the nonbait anchor fragment. Before calculating the $\log_2$ ratio, the raw counts of a loop were normalized to the total usable counts of the associated bait promoter. To plot PCHi-C data for a promoter in a 4C-like style (virtual 4C), data associated only with an individual promoter were extracted from the chinput file. A bedgraph file was generated using a custom script that incorporated the coordinates of each nonbait anchor fragment and the normalized PCHi-C counts. Virtual 4C data were visualized using the Washington University genome browser (http://epigenomegateway.wustl.edu/browser).

Data availability

The accession number for the sequencing data is GSE178852.

Competing interest statement

The authors declare no competing interests.

Acknowledgments

We thank Iris Dror and Amanda Collier for helpful discussion on promoter capture Hi-C analyses. We also thank Yu Sun and An-Chieh Feng for their suggestions on the manuscript preparation. This study was supported by the National Institutes of Health grant R01 GM074701 to M.F.C. C.H. was supported by the National Natural Science Foundation of China (81671396), the Natural Science Foundation of Guangdong Province (2017A030313780), and the Science and Technology Project of Shantou (2019ST006). M.K. was supported by a Ruth L. Kirschstein National Research Service Award (GM007185).

Author contributions: F.S. and M.F.C conceived and designed the experiments. F.S. performed all of the experiments and bioinformatic analyses. T.S. assisted in library construction, qPCR analyses, and generation of plasmids for the shRNA screen. M.K. assisted in total RNA extraction for the shRNA screen. X.T. helped in generating the Supplemental Tables. C.H. assisted on strategy and in promoter capture Hi-C sequencing. F.S. and M.F.C wrote the manuscript.

References

Abdella R, Talyzina A, Chen S, Inouye CJ, Tjian R, He Y. 2021. Structure of the human Mediator-bound transcription preinitiation complex. *Science* **372:** 52–56. doi:10.1126/science.abg3074

Baptista T, Grünberg S, Minoungou N, Koster MJE, Timmers HTM, Hahn S, Devys D, Tora L. 2017. SAGA is a general cofactor for RNA polymerase II transcription. *Mol Cell* **68:** 130–143.e5. doi:10.1016/j.molcel.2017.08.016

Bhuiyan T, Timmers HTM. 2019. Promoter recognition: putting TFIID on the spot. *Trends Cell Biol* **29:** 752–763. doi:10.1016/j.tcb.2019.06.004

Bourbon HM. 2008. Comparative genomics supports a deep evolutionary origin for the large, four-module transcriptional mediator complex. *Nucleic Acids Res* **36:** 3993–4008. doi:10.1093/nar/gkn349

Buratowski S, Hahn S, Guarente L, Sharp PA. 1989. Five intermediate complexes in transcription initiation by RNA polymerase II. *Cell* **56:** 549–561. doi:10.1016/0092-8674(89)90578-3

Burrows JTA, Pearson BJ, Scott IC. 2015. An in vivo requirement for the mediator subunit Med14 in the maintenance of stem cell populations. *Stem Cell Reports* **4:** 670–684. doi:10.1016/j.stemcr.2015.02.006

Cairns J, Freire-Pritchett P, Wingett SW, Várnai C, Dimond A, Plagnol V, Zerbino D, Schoenfelder S, Javierre BM, Osborne C, et al. 2016. CHiCAGO: robust detection of DNA looping interactions in capture Hi-C data. *Genome Biol* **17:** 127. doi:10.1186/s13059-016-0992-2

Cevher MA, Shi Y, Li D, Chait BT, Malik S, Roeder RG. 2014. Reconstitution of active human core mediator complex reveals a critical role of the MED14 subunit. *Nat Struct Mol Biol* **21:** 1028–1034. doi:10.1038/nsmb.2914

Chen XF, Lehmann L, Lin JJ, Vashisht A, Schmidt R, Ferrari R, Huang C, McKee R, Mosley A, Plath K, et al. 2012. Mediator and SAGA have distinct roles in Pol II preinitiation complex assembly and function. *Cell Rep* **2:** 1061–1067. doi:10.1016/j.celrep.2012.10.019

Chi T, Lieberman P, Ellwood K, Carey M. 1995. A general mechanism for transcriptional synergy by eukaryotic activators. *Nature* **377:** 254–257. doi:10.1038/377254a0

Chronis C, Fiziev P, Papp B, Butz S, Bonora G, Sabri S, Ernst J, Plath K. 2017. Cooperative binding of transcription factors orchestrates reprogramming. *Cell* **168:** 442–459.e20. doi:10.1016/j.cell.2016.12.016

Dao LTM, Galindo-Albarrán AO, Castro-Mondragon JA, Andrieu-Soler C, Medina-Rivera A, Souaid C, Charbonnier G, Griffon A, Vanhille L, Stephen T, et al. 2017. Genome-wide characterization of mammalian promoters with distal enhancer functions. *Nat Genet* **49:** 1073–1081. doi:10.1038/ng.3884

Dignam JD, Lebovitz RM, Roeder RG. 1983. Accurate transcription initiation by RNA polymerase II in a soluble extract from isolated mammalian nuclei. *Nucleic Acids Res* **11:** 1475–1489. doi:10.1093/nar/11.5.1475

Donczew R, Warfield L, Pacheco D, Erijman A, Hahn S. 2020. Two roles for the yeast transcription coactivator SAGA and a set of genes redundantly regulated by TFIID and SAGA. *Elife* **9:** e50109. doi:10.7554/eLife.50109

El Khattabi L, Zhao H, Kalchschmidt J, Young N, Jung S, Van Blerkom P, Kieffer-Kwon P, Kieffer-Kwon KR, Park S, Wang X, et al. 2019. A pliable Mediator acts as a functional rather than an architectural bridge between promoters and enhancers. *Cell* **178:** 1145–1158.e20. doi:10.1016/j.cell.2019.07.011

Grünberg S, Henikoff S, Hahn S, Zentner GE. 2016. Mediator binding to UAS s is broadly uncoupled from transcription and cooperative with TFIID recruitment to promoters. *EMBO J* **35:** 2435–2446. doi:10.15252/embj.201695020

Hirsch CL, Akdemir ZC, Wang L, Jayakumaran G, Trcka D, Weiss A, Hernandez JJ, Pan Q, Han H, Xu X, et al. 2015. Myc and SAGA rewire an alternative splicing network during early somatic cell reprogramming. *Genes Dev* **29:** 803–816. doi:10.1101/gad.255109.114

Holstege FCP, Van Der Vliet PC, Timmers HTM. 1996. Opening of an RNA polymerase II promoter occurs in two distinct steps and requires the basal transcription factors IIE and IIH. *EMBO J* **15:** 1666–1677. doi:10.1002/j.1460-2075.1996.tb00512.x

Hsieh CL, Fei T, Chen Y, Li T, Gao Y, Wang X, Sun T, Sweeney CJ, Lee GSM, Chen S, et al. 2014. Enhancer RNAs participate in androgen receptor-driven looping that selectively enhances gene activation. *Proc Natl Acad Sci* **111:** 7319–7324. doi:10.1073/pnas.1324151111

Jaeger MG, Schwalb B, Mackowiak SD, Velychko T, Hanzl A, Imrichova H, Brand M, Agerer B, Chorn S, Nabet B, et al. 2020. Selective Mediator dependence of cell-type-specifying transcription. *Nat Genet* **52:** 719–727. doi:10.1038/s41588-020-0635-0

Jiang Y, Huang J, Lun K, Li B, Zheng H, Li Y, Zhou R, Duan W, Feng Y, Yao H, et al. 2020. Genome-wide analyses of chromatin interactions after the loss of Pol I, Pol II and Pol III. *Genome Biol* **21:** 158. doi:10.1186/s13059-020-02067-3

Johnson KM, Carey M. 2003. Assembly of a mediator/TFIID/TFIIA complex bypasses the need for an activator. *Curr Biol* **13:** 772–777. doi:10.1016/S0960-9822(03)00283-5

Johnson KM, Wang J, Smallwood A, Arayata C, Carey M. 2002. TFIID and human mediator coactivator complexes assemble cooperatively on promoter DNA. *Genes Dev* **16:** 1852–1863. doi:10.1101/gad.995702

Jung I, Schmitt A, Diao Y, Lee AJ, Liu T, Yang D, Tan C, Eom J, Chan M, Chee S, et al. 2019. A compendium of promoter-centered long-range chromatin interactions in the human genome. *Nat Genet* **51:** 1442–1449. doi:10.1038/s41588-019-0494-8

Kagey MH, Newman JJ, Bilodeau S, Zhan Y, Orlando DA, Van Berkum NL, Ebmeier CC, Goossens J, Rahl PB, Levine SS, et al. 2010. Mediator and cohesin connect gene expression and chromatin architecture. *Nature* **467:** 430–435. doi:10.1038/nature09380

Kim YJ, Björklund S, Li Y, Sayre MH, Kornberg RD. 1994. A multiprotein mediator of transcriptional activation and its interaction with the C-terminal repeat domain of RNA polymerase II. *Cell* **77:** 599–608. doi:10.1016/0092-8674(94)90221-6

Koch F, Fenouil R, Gut M, Cauchy P, Albert TK, Zacarias-Cabeza J, Spicuglia S, De La Chapelle AL, Heidemann M, Hintermair C, et al. 2011. Transcription initiation platforms and GTF recruitment at tissue-specific enhancers and promoters. *Nat Struct Mol Biol* **18:** 956–963. doi:10.1038/nsmb.2085

Kostrewa D, Zeller ME, Armache KJ, Seizl M, Leike K, Thomm M, Cramer P. 2009. RNA polymerase II-TFIIB structure and mechanism of transcription initiation. *Nature* **462:** 323–330. doi:10.1038/nature08548

Krivega I, Dean A. 2017. LDB1-mediated enhancer looping can be established independent of mediator and cohesin. *Nucleic Acids Res* **45:** 8255–8268. doi:10.1093/nar/gkx433

Kuras L, Struhl K. 1999. Binding of TBP to promoters in vivo is stimulated by activators and requires Pol II holoenzyme. *Nature* **399:** 609–613. doi:10.1038/21239

Li W, Notani D, Ma Q, Tanasa B, Nunez E, Chen AY, Merkurjev D, Zhang J, Ohgi K, Song X, et al. 2013. Functional roles of enhancer RNAs for oestrogen-dependent transcriptional activation. *Nature* **498:** 516–520. doi:10.1038/nature12210

Lin W, Srajer G, Evrard YA, Phan HM, Furuta Y, Dent SYR. 2007. Developmental potential of $Gcn5^{-/-}$ embryonic stem cells in vivo and in vitro. *Dev Dyn* **236:** 1547–1557. doi:10.1002/dvdy.21160

Liu Z, Scannell DR, Eisen MB, Tjian R. 2011. Control of embryonic stem cell lineage commitment by core promoter factor, TAF3. *Cell* **146:** 720–731. doi:10.1016/j.cell.2011.08.005

Louder RK, He Y, López-Blanco JR, Fang J, Chacón P, Nogales E. 2016. Structure of promoter-bound TFIID and model of human pre-initiation complex assembly. *Nature* **531:** 604–609. doi:10.1038/nature17394

Natsume T, Kiyomitsu T, Saga Y, Kanemaki MT. 2016. Rapid protein depletion in human cells by auxin-inducible degron tagging with short homology donors. *Cell Rep* **15:** 210–218. doi:10.1016/j.celrep.2016.03.001

Nora EP, Goloborodko A, Valton AL, Gibcus JH, Uebersohn A, Abdennur N, Dekker J, Mirny LA, Bruneau BG. 2017. Targeted degradation of CTCF decouples local insulation of chromosome domains from genomic compartmentalization. *Cell* **169:** 930–944.e22. doi:10.1016/j.cell.2017.05.004

Papai G, Frechard A, Kolesnikova O, Crucifix C, Schultz P, Ben-Shem A. 2020. Structure of SAGA and mechanism of TBP deposition on gene promoters. *Nature* **577:** 711–716. doi:10.1038/s41586-020-1944-2

Patel AB, Louder RK, Greber BJ, Grünberg S, Luo J, Fang J, Liu Y, Ranish J, Hahn S, Nogales E. 2018. Structure of human TFIID and mechanism of TBP loading onto promoter DNA. *Science* **362:** eaau8872. doi:10.1126/science.aau8872

Phillips-Cremins JE, Sauria MEG, Sanyal A, Gerasimova TI, Lajoie BR, Bell JSK, Ong CT, Hookway TA, Guo C, Sun Y, et al. 2013. Architectural protein subclasses shape 3D organization of genomes during lineage commitment. *Cell* **153:** 1281–1295. doi:10.1016/j.cell.2013.04.053

Pijnappel WWMP, Esch D, Baltissen MPA, Wu G, Mischerikow N, Bergsma AJ, Van Der Wal E, Han DW, Bruch HV, Moritz S, et al. 2013. A central role for TFIID in the pluripotent transcription circuitry. *Nature* **495:** 516–519. doi:10.1038/nature11970

Plaschka C, Larivière L, Wenzeck L, Seizl M, Hemann M, Tegunov D, Petrotchenko EV, Borchers CH, Baumeister W, Herzog F, et al. 2015. Architecture of the RNA polymerase II–Mediator core initiation complex. *Nature* **518:** 376–380. doi:10.1038/nature14229

Rao SSP, Huntley MH, Durand NC, Stamenova EK, Bochkov ID, Robinson JT, Sanborn AL, Machol I, Omer AD, Lander ES, et al. 2014. A 3D map of the human genome at kilobase resolution reveals principles of chromatin looping. *Cell* **159:** 1665–1680. doi:10.1016/j.cell.2014.11.021

Rao SSP, Huang SC, Glenn St Hilaire B, Engreitz JM, Perez EM, Kieffer-Kwon KR, Sanborn AL, Johnstone SE, Bascom GD, Bochkov ID, et al. 2017. Cohesin loss eliminates all loop domains. *Cell* **171:** 305–320.e24. doi:10.1016/j.cell.2017.09.026

Sato S, Tomomori-Sato C, Parmely TJ, Florens L, Zybailov B, Swanson SK, Banks CAS, Jin J, Cai Y, Washburn MP, et al. 2004. A set of consensus mammalian mediator subunits identified by multidimensional protein identification technology. *Mol Cell* **14:** 685–691. doi:10.1016/j.molcel.2004.05.006

Soutourina J. 2018. Transcription regulation by the mediator complex. *Nat Rev Mol Cell Biol* **19:** 262–274. doi:10.1038/nrm.2017.115

Sun F, Chronis C, Kronenberg M, Chen XF, Su T, Lay FD, Plath K, Kurdistani SK, Carey MF. 2019. Promoter–enhancer communication occurs primarily within insulated neighborhoods. *Mol Cell* **73:** 250–263.e5. doi:10.1016/j.molcel.2018.10.039

Takahashi H, Parmely TJ, Sato S, Tomomori-Sato C, Banks CAS, Kong SE, Szutorisz H, Swanson SK, Martin-Brown S, Washburn MP, et al. 2011. Human mediator subunit MED26 functions as a docking site for transcription elongation factors. *Cell* **146:** 92–104. doi:10.1016/j.cell.2011.06.005

Tsai KL, Yu X, Gopalan S, Chao TC, Zhang Y, Florens L, Washburn MP, Murakami K, Conaway RC, Conaway JW, et al. 2017. Mediator structure and rearrangements required for holoenzyme formation. *Nature* **544:** 196–201. doi:10.1038/nature21393

Whyte WA, Orlando DA, Hnisz D, Abraham BJ, Lin CY, Kagey MH, Rahl PB, Lee TI, Young RA. 2013. Master transcription factors and mediator establish super-enhancers at key cell identity genes. *Cell* **153:** 307–319. doi:10.1016/j.cell.2013.03.035

Wingett SW, Ewels P, Furlan-Magaril M, Nagano T, Schoenfelder S, Fraser P, Andrews S. 2015. HiCUP: pipeline for mapping and processing Hi-C data. *F1000Res* **4:** 1310. doi:10.12688/f1000research.7334.1

Wright KJ, Marr MT, Tjian R. 2006. TAF4 nucleates a core subcomplex of TFIID and mediates activated transcription from a TATA-less promoter. *Proc Natl Acad Sci* **103:** 12347–12352. doi:10.1073/pnas.0605499103

Xu Y, Milazzo JP, Somerville TDD, Tarumoto Y, Huang YH, Ostrander EL, Wilkinson JE, Challen GA, Vakoc CR. 2018. A TFIID-SAGA perturbation that targets MYB and suppresses acute myeloid leukemia. *Cancer Cell* **33:** 13–28.e8. doi:10.1016/j.ccell.2017.12.002

Zhao H, Young N, Kalchschmidt J, Lieberman J, El Khattabi L, Casellas R, Asturias FJ. 2021. Structure of mammalian mediator complex reveals tail module architecture and interaction with a conserved core. *Nat Commun* **12:** 1355. doi:10.1038/s41467-021-21601-w

Zhou HY, Katsman Y, Dhaliwal NK, Davidson S, Macpherson NN, Sakthidevi M, Collura F, Mitchell JA. 2014. A *Sox2* distal enhancer cluster regulates embryonic stem cell differentiation potential. *Genes Dev* **28:** 2699–2711. doi:10.1101/gad.248526.114